

Modelling Soil $\delta^{13}\text{C}$ across the Tibetan Plateau Using Deep-Learning

T. Zhou^{1, 2*}, Y. S. Lai^{1*}, Z. H. Yang¹, Y. H. Shi¹, X. R. Luo¹, L. Liu¹, P. Yu¹, G. Chen², L. X. Cao², S. H. Fan³, C. J. Cai³, J. Sun⁴, S. H. Chen⁵, H. Y. Lu^{6, 7, 8}, X. L. Ma⁹, S. D. Li¹, and X. L. Tang^{2, 10, 11**}

¹ College of Earth Science, Chengdu University of Technology, Chengdu 610059, China

² College of Ecology and Environment, Chengdu University of Technology, Chengdu 610059, China

³ Key Laboratory of Bamboo and Rattan Science and Technology of National Forestry and Grassland Administration, International Centre for Bamboo and Rattan, Beijing 100102, China

⁴ Key Laboratory of Alpine Ecology, Institute of Tibetan Plateau Research, Chinese Academy of Sciences, Beijing 100101, China

⁵ Key Laboratory of Water Cycle and Related Land Surface Processes, Institute of Geographic Sciences and Natural Resources Research, Chinese Academy of Sciences, Beijing 100101, China

⁶ Center for Excellence in Tibetan Plateau Earth Science, Chinese Academy of Sciences, Beijing 100101, China

⁷ University of Chinese Academy of Sciences, Beijing 100049, China

⁸ Key Laboratory of Cenozoic Geology and Environment, Institute of Geology and Geophysics, Chinese Academy of Sciences, Beijing 100029, China

⁹ College of Earth and Environmental Sciences, Lanzhou University, Lanzhou 730000, China

¹⁰ State Key Laboratory of Geohazard Prevention and Geoenvironment Protection, Chengdu University of Technology, Chengdu 610059, China

¹¹ Tianfu Yongxing Laboratory, Chengdu 610059, China

Received 30 January 2023; revised 31 March 2023; accepted 06 January 2024; published online 30 June 2024

ABSTRACT. Soil carbon isotopes ($\delta^{13}\text{C}$) provide reliable insights for studying soil carbon turnover at a long-term scale. The Tibetan Plateau (TP), often referred as “the third pole of the earth”, is highly sensitive to global climate change, and exhibits an early warning signal of global warming. Although many studies detected soil $\delta^{13}\text{C}$ variability at site scales, there is still a knowledge gap existing in the spatial pattern of soil $\delta^{13}\text{C}$ across the TP. In this study, we compiled a database of 198 topsoil $\delta^{13}\text{C}$ observations from published literatures and used a modified multi-layer perceptron (MLP) neural network algorithm to predict the spatial pattern of topsoil $\delta^{13}\text{C}$ and β (indicating the decomposition rate of soil organic carbon (SOC), calculated as $\delta^{13}\text{C}$ divided by logarithmically converted SOC) at 500 m resolution. Results showed that MLP model effectively predicted topsoil $\delta^{13}\text{C}$ with a model efficiency of 0.72 and a root mean square error of 1.16‰. Topsoil $\delta^{13}\text{C}$ varied significantly across different ecosystem types ($p < 0.001$) with a mean $\delta^{13}\text{C}$ of $-25.89 \pm 1.15\text{‰}$ (mean \pm standard deviation) for forests, $-24.91 \pm 1.03\text{‰}$ for shrublands, $-22.95 \pm 1.44\text{‰}$ for grasslands, and $-18.88 \pm 2.37\text{‰}$ for deserts. Furthermore, there was an increasing trend of predicted $\delta^{13}\text{C}$ from the southeastern to the northwestern TP, likely linked to vegetation type and climatic conditions. β values were low in the eastern TP and higher in the northern and northwestern TP, indicating faster SOC turnover rate in the east TP compared to the north and northwest. This study represents the first effort to develop a fine resolution product of topsoil $\delta^{13}\text{C}$ and β across the TP, which could provide an independent, data-driven benchmark for biogeochemical cycling models to study SOC turnover and terrestrial carbon-climate feedback over the TP under climate change.

Keywords: soil $\delta^{13}\text{C}$, spatial variability, multi-layer perceptron neural network, soil carbon turnover, Tibetan Plateau, biogeochemical cycles

1. Introduction

Soil organic carbon (SOC) is the largest carbon pool in terrestrial ecosystems, containing about 1500 Pg C (1 Pg C = 10^{15} grams of carbon) within the first meter, which is two-fold higher than that of the atmosphere (Bateni et al., 2014; Scharlemann et al., 2014). Due to the decomposition of SOC, an amount of 57.2 Pg C was released from the soil to the atmosphere (Tang et al., 2020). Thus, a small change in SOC can have a profound

impact on the atmospheric CO_2 (carbon dioxide) concentrations and consequently climate change (Köchy et al., 2015). Detecting statistically significant changes in SOC pool over a short time is challenging (Groenigen et al., 2014). Therefore, understanding SOC dynamics is crucial for assessing ecosystem carbon balance and its feedback to climate change (Campbell et al., 2009; Wang et al., 2012; Averill et al., 2014).

Carbon isotopes ($\delta^{13}\text{C}$) in SOC provide reliable insights for studying long-term soil carbon turnover (Khan et al., 2008; Blagodataskaya et al., 2011; Acton et al., 2013; Li et al., 2020). As the majority of SOC originates from plant residues, soil $\delta^{13}\text{C}$ reflects vegetation-related soil formation and dynamics (Ehleringer et al., 2000). Previous studies have mainly focused on the spatial variability of soil $\delta^{13}\text{C}$ at in-site scales (Lu et al.,

* Co-first authors

** Corresponding author. Tel.: 176-1115-9509, fax: 86-028-84073434
E-mail address: lxtt2010@163.com (X. L. Tang).

2004; Wang et al., 2012; Acton et al., 2013). For example, it is widely observed that soil $\delta^{13}\text{C}$ values increase with increasing soil depth and decreasing SOC (Wang et al., 2012; Brunn et al., 2014; Gautam et al., 2017; Wang et al., 2017). Meanwhile, climate, edaphic variables, and their combinations have a vital influence on the spatial variability of soil $\delta^{13}\text{C}$ (Garten et al., 2000). However, modeling the spatial patterns of $\delta^{13}\text{C}$ using field observations has not been observed. Recent studies highlighted the importance of understanding soil $\delta^{13}\text{C}$ variability at a regional scale for insights into soil carbon dynamics and climate change feedback (Rao et al., 2017; Zhao et al., 2019; Li et al., 2020). Therefore, there is an urgent need for a high-precision, high-resolution, and large-scale $\delta^{13}\text{C}$ estimation method to comprehensively understand the spatial patterns of SOC.

Previous studies have identified a negative linear correlation between the log-transformed SOC concentration and soil $\delta^{13}\text{C}$ (Garten et al., 2006; Acton et al., 2013). The slope of the linear regression of soil $\delta^{13}\text{C}$ on log-transformed organic carbon concentration is defined as β , a proxy of SOC decomposition (Garten, 2006). A more negative slope indicates a larger decrease in β and a faster turnover rate (Campbell et al., 2009). This method has been widely used to study SOC turnover across forest, grassland, and meadow ecosystems (Peri et al., 2012; Gautam et al., 2017; Zhao et al., 2019; Zhou et al., 2019). Acton et al. (2013) noted that β is applicable to well-drained soils characterized by a gradual mixing of litter and root carbon inputs decomposing in the soil profile. Furthermore, empirical studies have highlighted the significance of temperature, precipitation, and soil properties in driving β (Wynn et al., 2006). However, these factors exhibit substantial variability across climate zones and biomes, suggesting a strong spatial pattern of β . Therefore, understanding the spatial patterns of β is crucial for studying SOC turnover time and its sensitivity to climate. Yet, the extent to which β values can rates and controls on SOC turnover remains underexplored at regional scales, particularly for the TP.

Soil $\delta^{13}\text{C}$ is a crucial indicator of SOC dynamics. It has been mostly observed at the sample scale (Julian Martinon-Martinez et al., 2011; Bogino et al., 2014; Carvalho et al., 2017). The commonly used methods to calculate soil $\delta^{13}\text{C}$ can be divided into two categories: natural marker methods and artificial marker methods (Liu et al., 2008). These methods are known for their high accuracy but suffer from high labor cost and limited spatial data extrapolation (Sun et al., 2021). As a result, the spatial patterns and turnover characteristics of SOC based on soil $\delta^{13}\text{C}$ at regional scale remain unclear, especially in the sensitive TP region. In regional-scale simulations, carbon cycle models including Century model (Parton et al., 1987), Community land model (Lawrence et al., 2019), Terrestrial ecosystem model (Liang et al., 2018), and Michaelis-Menten necromass decomposition model (Fan et al., 2021) are key tools in predicting SOC responses to future climate change. However, there are significant uncertainties in simulating and predicting SOC cycle using numerical Earth system models. These uncertainties arise from challenges in quantifying crucial parameters and the inherent complexity of the models (Shi et al., 2018; Zhou et al., 2022). Recently, machine learning approaches, notably MLP (Jin et al., 1997), have gained popularity in the fields of ecology and Earth

sciences. In particular, these approaches have been useful in leveraging variables to establish relationships between target variables and predictive variables (Mattei et al., 2020; Tang et al., 2020; Singhal et al., 2021). Data-driven MLP models have fewer parameters and are more easily accessible (Yang et al., 2023). Thus, the increasing availability of field observations, combined with the advancements in deep learning models, provides an excellent opportunity to narrow the knowledge gap for the evaluation of spatial variability in soil $\delta^{13}\text{C}$ and β .

The TP is the world largest and highest plateau with an average elevation of more than 4000 m above sea level and covers about $2.5 \times 10^6 \text{ km}^2$ (Lu et al., 2004). Soils in the TP store about 4.4 Pg C within 30 cm (Yang et al., 2009), accounting for 12.4 % of total SOC in China's grasslands (Fang et al., 2010). In the last few decades, surface air temperature in the TP has increased by 0.44 °C per decade, which was almost three times the world average (0.16 °C per decade) (Duan et al., 2015). Site-level studies found that the decomposition rate of SOC accelerates with temperature increase, resulting in the release of stored carbon from the soil into the atmosphere (Chang et al., 2012; Dong et al., 2018; Li et al., 2019). However, regional estimates of the sensitivity of SOC decomposition in the TP are still missing, and knowledge gaps still exist in the spatial patterns of soil $\delta^{13}\text{C}$, SOC turnover (β) and their driving mechanisms. Therefore, it is crucial to have a comprehensive understanding of SOC turnover and the dynamic mechanisms that influence SOC in order to accurately assess SOC dynamics in high altitude areas.

In this study, we first compiled a database of topsoil $\delta^{13}\text{C}$ obtained from published literature based on field observations from the TP. We then applied an MLP neural network algorithm to predict the spatial patterns of topsoil $\delta^{13}\text{C}$ by linking environment variables. The objectives of this study are to: (1) compare the $\delta^{13}\text{C}$ across different ecosystems; (2) model the spatial variability of topsoil $\delta^{13}\text{C}$ and β ; (3) explore their driving mechanisms over the TP.

2. Material and Methods

2.1. Data Sources

The topsoil (0 ~ 3 cm) $\delta^{13}\text{C}$ dataset primarily originates from the study by Lu et al. (2004), which contained 198 field observations (Figure 1). These field observations were collected along different elevation gradients at approximately 50 ~ 70 km sampling intervals, and leaves, roots, and litter were removed before sampling (Lu et al., 2004). All observations were dried at 60 °C and grounded to less than 250 μm , and then pretreatment experiments to remove carbonates. Subsequently, topsoil $\delta^{13}\text{C}$ was measured for carbon isotope ratios using an NC2500 (EAIRMS) mass spectrometer. Lu et al. (2004) indicated less than with an overall analytical accuracy of 0.1‰. Furthermore, 28 duplicate samples from different soil sediments were repeatedly analyzed with an average deviation of 0.23‰, which indicated that the dataset was reliable and stable. Finally, the database included 16 observations from deserts, 23 observations from forests, 130 observations from grasslands, and 29 observations from shrublands. More comprehensive information, such as data coordinates and sources, was included in the C13_3cm.csv file under Data availability.

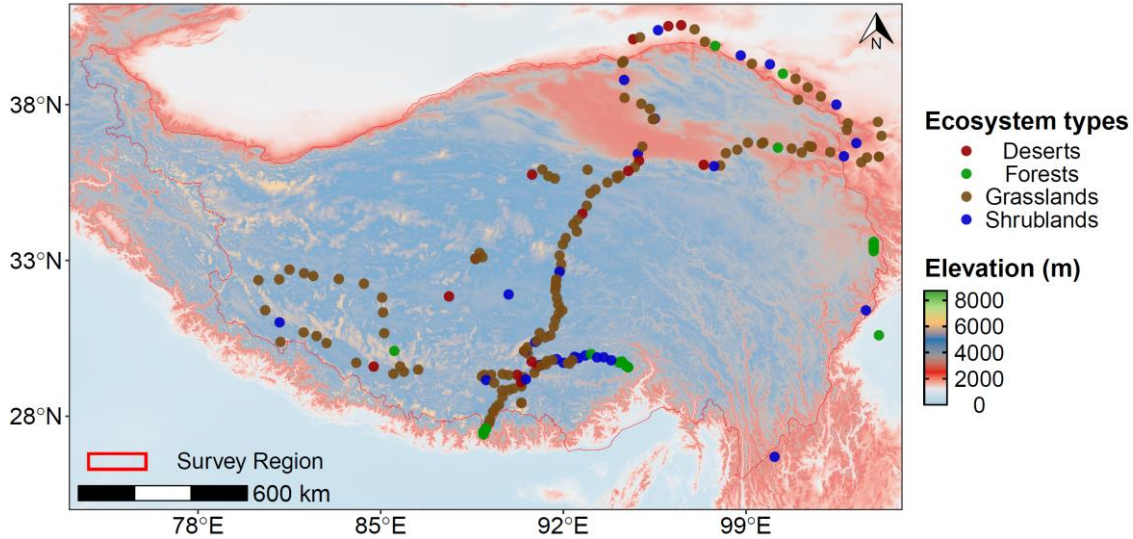


Figure 1. The distributions of the study sites.

2.2. Environmental Variables

Topsoil $\delta^{13}\text{C}$ is affected by multiple environmental factors. To investigate the spatial patterns of $\delta^{13}\text{C}$, the spatial grid of environmental variables was required. The environmental variables included: mean annual 2 m dewpoint and mean annual skin temperature (MAT), mean annual surface pressure (SP), annual total evaporation (ET), and annual total precipitation (MAP) with a spatial resolution of 11,132 m from ERA5-Land monthly averaged data (Muñoz Sabater, 2019). Moderate-resolution Imaging Spectroradiometer (MODIS) products were obtained from <https://lpdaac.usgs.gov>, including normalized difference vegetation index (NDVI) and enhanced vegetation index (EVI) with a spatial resolution of 250 m (Didan, 2021), leaf area index (LAI) (Myneni et al., 2021), fraction of photosynthetically active radiation (FPAR) (Myneni et al., 2021), and land cover type (LC) (Friedl et al., 2022) with a spatial resolution of 500 m, and land surface temperature (LST) with a spatial resolution of 1000 m (Wan et al., 2021). Gross primary productivity (GPP), vegetation transpiration (EC), soil evaporation (ES) and interception from vegetation canopy (EI) were obtained from PML V2 0.1.7, with a spatial resolution of 500 m (Zhang et al., 2019). Soil variables (e.g., soil organic content (SOC) and soil clay content (CLAY)) were obtained from the SoilGrids database with spatial resolution of 250 m (Hengl et al., 2017). Elevation data (digital elevation map; DEM) were obtained from Yamazaki et al. (2017) with a spatial resolution of 90 m. Soil water content (SWC) at 10 cm depth was obtained from Hengl et al., (2019) with a spatial resolution of 500 m. These variables were downloaded using the Google Earth Engine platform (Gorelick et al., 2017). Due to the limitations of data availability, the download date for some variables, such as LC, NDVI, LST, and others, corresponds to the latest available year. If the predicting variables were not in a spatial resolution of 500 m, these variables were resampled to 500 m using the bilinear interpolation approach. Furthermore, the full names of all abbreviations used in this paper are presented in Table 1.

2.3. Data Analysis

One-way analysis of variance (ANOVA) was performed to analyze the significant difference of soil $\delta^{13}\text{C}$ in forests, shrublands, grasslands, and deserts. When significance was observed at the $p < 0.05$ level, we applied the Tukey-HSD (honestly significant difference) for multiple comparisons. The Tukey-HSD is a post-hoc test based on the studentized range distribution that determines which specific groups' means are different by comparing all possible pairs of means (Bretz et al., 2010). The correlation analysis was conducted to explore the relationships between topsoil $\delta^{13}\text{C}$ and climate, vegetations, and soil factors.

The β values, which reflect the sensitivity of SOC decomposition (Garten, 2006), were obtained using a standard least-squares regression analysis between the log₁₀-transformed SOC concentration and $\delta^{13}\text{C}$:

$$\delta^{13}\text{C}_{\text{SOC}} = \beta \times \log(\text{SOC}) + \alpha \quad (1)$$

Where $\delta^{13}\text{C}_{\text{SOC}}$ is the $\delta^{13}\text{C}$ in SOC, β is the regression coefficient, and α is a constant number, which was obtained using a standard-least squares regression analysis between the log₁₀ transformed SOC concentration and soil $\delta^{13}\text{C}$ from gathering dataset (Figure S1). In current study, the SOC within 0 ~ 5 cm from SoilGrids was used (Hengl et al., 2017). All the analyses were conducted in R 4.2.1 (R Core Team, 2022).

2.4. Spatial Modeling

2.4.1. Feature Selection

In order to improve the model efficiency and reduce the workload, an Explanatory Model Analysis (EMA) algorithm was used for variable selection (Lipovetsky, 2022). This algorithm assesses the loss of Root Mean Square Error (RMSE) to measure how a model's performance would change if the effect of one variable is removed. We repeated the process ten times

using ten permutations to compute the mean values of RMSE loss, treating it as one variable importance. For this purpose, we used the *DALEX R* package. The EMA algorithm combines recursive methods to select features, starting with all input variables participating in MLP modeling based on their importance ranking. It then gradually removes the least important indicators from the current feature set, creating a new MLP with the reduced feature set. This process repeats until best features remained. Finally, based on this approach, we selected MAP, MAT, LST, EI, ET, SWC, and OCS to predict soil $\delta^{13}\text{C}$. The relative importance evaluation of all the variables is shown in Figure S2.

Table 1. Full Name for All Abbreviations

Abbreviations	Full Name	Unit
TP	The Tibetan Plateau	-
SOC	Soil Organic Carbon	Pg C
$\delta^{13}\text{C}$	Carbon Isotopes of Soil Organic Carbon	%
β	The Decomposition Rate of Soil Organic Carbon (SOC)	-
MAT	Annual Skin Temperature	$^{\circ}\text{C}$
SP	Annual Surface Pressure	Pa
ET	Evaporation	mm
MAP	Precipitation	mm
NDVI	Normalized Difference Vegetation Index	-
EVI	Enhanced Vegetation Index	-
LAI	Leaf Area Index	%
FPAR	Fraction of Photosynthetically Active Radiation	%
LC	Land Cover Type	-
LST	Land Surface Temperature	$^{\circ}\text{C}$
GPP	Gross Primary Productivity	$\text{g C m}^{-2} \text{d}^{-1}$
EC	Vegetation	mm
ES	Soil Evaporation	mm
EI	Interception From Vegetation Canopy	mm
CLAY	Soil Clay Content	g kg^{-1}
OCS	Soil Organic Carbon Stock	t ha^{-1}
CEC	Cation-Exchange Capacity	mmol(c) kg^{-1}
SILT	Silt Content	g kg^{-1}
CFVO	Coarse Fragments Volumetric	$\text{cm}^3 \text{dm}^{-3}$
SAND	Soil Sand Content	g kg^{-1}
BDOD	Soil Bulk Density	cg cm^{-3}
DEM	Digital Elevation Map	m
SWC	Soil Water Content At 10 cm Depth	%
MLP	The Multi-Layer Perceptron Neural Network	-
ANOVA	One-Way Analysis of Variance	-
Tukey-HSD	Honestly Significant Difference	-
EMA	The Explanatory Model Analysis Algorithm	-
RMSE	Root Mean Square Error	-

2.4.2. Modeling

MLP, known as a deep feedforward network, is a basic deep learning network structure with very good nonlinear mapping capabilities, high parallelism, and global optimization (Le-Cun et al., 2015; Gomez-Fernandez et al., 2021). For example, Jaber et al. (2011) demonstrated the potential of the deep feedforward network for total SOC pools in various ecosystem or soil types using remote sensing data. Kuang et al. (2015) demonstrated that neural networks outperform traditional partial least squares regression (PLSR) in the estimation of soil organic carbon (SOC), showing improved model efficiency and better spatial performance. Thus, MLP was chosen to model the spatial patterns of soil $\delta^{13}\text{C}$. However, its efficiency is relatively low in high-dimensional space, which may lead to overfitting in model training. To overcome these problems, our study used a modified MLP neural network model, incorporating 10-fold cross-validation and EMA algorithm (Bodesheim et al., 2018; Jian et al., 2018; Tang et al., 2020). This modified model boasts a simple structure, a limited number of input variables, and easy interpretation.

The MLP model in this study consists of one input layer, two hidden layers, and one output layer. The number of neurons in the input layer is determined based on the number of input variables. The first hidden layer contains 140 neurons, and the number of neurons in the second hidden layer is set to 40, while 40% of the hidden layer neurons are randomly drop during the training process to prevent overfitting of the model. The output layer contains only one neuron as the output of the regression prediction result. MLP models have two important custom parameters, Epoch (Number of model iterations) and Batch size (Number of samples selected for one training session). The optimal Epoch was chosen based on the minimum mean absolute error (mae) calculated from 10-fold cross-validation MLP over 300 iterations with the Batch size set to 7. The MLP model was trained by *keras_model* in the *tensorflow* package (version 2.90) in R.

To train the model and evaluate the performance of MLP, a 10-fold cross-validation was applied, which can avoid the constraints and peculiarities of fixed partition data sets, and this advantage is particularly visible on small-scale data sets (Singh et al., 2011). This involved stratifying the dataset into ten parts, each containing approximately an equal number of samples. The target values for each of these ten parts had predicted using a model trained on the remaining nine parts (Jung et al., 2011; Tang et al., 2019, 2020). The model efficiency (R^2) and *RMSE* were used for model evaluation (Yao et al., 2018; Tang et al., 2020; Zhou et al., 2023). The specific implementation steps were as follows: 1) The training dataset was constructed by extracting the environmental factor values from the location information of the site field observations of soil $\delta^{13}\text{C}$; 2) The model parameters were set, and the MLP model framework was constructed; 3) the degree of contribution of environmental factors to soil $\delta^{13}\text{C}$, i.e., variable importance, was determined and ranked using the EMA algorithm based on the constructed MLP model framework. The resulting dataset was then used as the input data for the model; 4) the training data set was split using the 10-

fold cross-validation method to generate ten distinct data subsets, each containing a validation set and a training set. These subsets were then input to the MLP model for 300 iterations. On this basis, the model with the best performance was determined, and its efficiency was evaluated; 5) The optimal model was used to predict soil $\delta^{13}\text{C}$ with a spatial resolution of 500 m, combining spatial variables factors.

3. Results

3.1. Soil $\delta^{13}\text{C}$ across Different Ecosystems

Large variabilities of topsoil $\delta^{13}\text{C}$ values were observed across different ecosystem types (Figure 2 and Table S1). Topsoil $\delta^{13}\text{C}$ ranged from -28.57‰ in forests to -15.08‰ in deserts, with a mean $\delta^{13}\text{C}$ of $-23.25 \pm 2.22\text{‰}$. In terms of ecosystem types, topsoil $\delta^{13}\text{C}$ varied significantly (Figure 2, $p < 0.001$). The highest $\delta^{13}\text{C}$ was $-18.88 \pm 2.37\text{‰}$ in deserts, followed by grasslands ($-22.95 \pm 1.44\text{‰}$), and shrublands ($-24.91 \pm 1.03\text{‰}$), with forests having the lowest $\delta^{13}\text{C}$ value ($-25.89 \pm 1.15\text{‰}$, Table S1). No significant difference in soil $\delta^{13}\text{C}$ was observed between forests and shrublands. Additionally, great variability was observed within the same ecosystem type. For example, topsoil $\delta^{13}\text{C}$ varied from -28.57‰ to -18.54‰ in grassland. The topsoil $\delta^{13}\text{C}$ of different ecosystems exhibited an increasing trend from forest to desert in the TP indicating that the topsoil was more enriched in soil $\delta^{13}\text{C}$ in desert, in the western regions. In contrast, the eastern regions, where the climate is relatively mild in forest, exhibited the lowest $\delta^{13}\text{C}$ content in the surface soil. Furthermore, we observed significant variability, with the highest values recorded within the desert ecosystems.

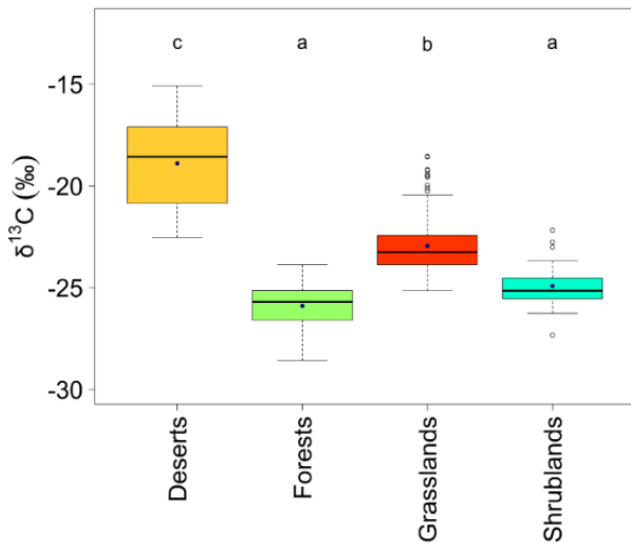


Figure 2. Boxplot of topsoil $\delta^{13}\text{C}$ across different ecosystem types. The blue dots represent the mean $\delta^{13}\text{C}$. The boxplot shows the median (line), first and third quartiles (box bounds), 1.5 times the interquartile (whiskers) and outliers (values outside of whisker limits) for each ecosystem type. Different low-ercase letters (a, b, and c) indicate significantly different ratios at $p < 0.05$ using one-way analysis of variance (ANOVA) and Tukey-HSD test for multiple comparisons.

3.2. Relationships between Soil $\delta^{13}\text{C}$ and Environmental Factors

Significant positive correlations were found between soil $\delta^{13}\text{C}$ and land surface temperature, soil evaporation, landcover, and soil bulk density. Conversely, significant negative correlations were observed between soil $\delta^{13}\text{C}$ and mean annual precipitation, mean annual 2 m dewpoint temperature, soil organic carbon stock, soil water content at 10 cm, cation-exchange capacity, interception from vegetation canopy, and vegetation transpiration (Figure 3, all $p_s < 0.05$). Additionally, interception from vegetation canopy, soil organic carbon stock, and cation-exchange capacity was identified as important variables, showing significant correlations with other climate and soil variables (all $p_s < 0.05$). On the contrary, some variables were found to be less important, showing insignificant correlations with soil silt, soil clay, soil sand, bulk density, and evaporation.

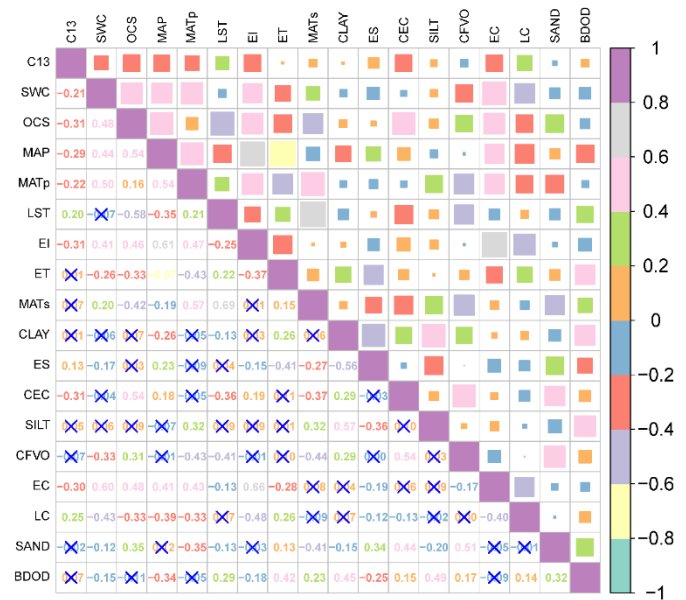


Figure 3. Pearson correlation coefficient between soil $\delta^{13}\text{C}$ and environmental factors. The numbers marked by 'x' indicate insignificance at the level of $p < 0.05$. C13: soil $\delta^{13}\text{C}$ (‰); MAT: mean annual 2 m dewpoint temperature ($^{\circ}\text{C}$); MAP: mean annual precipitation (mm); ET: annual evapotranspiration (mm); EI: interception from vegetation canopy (mm); ES: soil evaporation (mm); EC: vegetation transpiration (mm); LC: landcover; LST: land surface temperature ($^{\circ}\text{C}$); SWC: 10 cm depth of soil water content (%); OCS: soil organic carbon stock (t ha^{-1}); CLAY: soil clay content (g kg^{-1}); CEC: cation-exchange capacity (mmol(c) kg^{-1}); SILT: silt content (g kg^{-1}); CFVO: coarse fragments volumetric ($\text{cm}^3 \text{dm}^{-3}$); SAND: soil sand content (g kg^{-1}); BDOD: soil bulk density (cg cm^{-3}). The color bar represented different correlation ranges with different colors, the correlation range was standardized from -1 to 1.

3.3. Spatial Patterns of Topsoil $\delta^{13}\text{C}$ and β across the TP

Based on the 10-fold cross-validation, R^2 and $RMSE$ were

0.72 and 1.16%, respectively, indicating that MLP had the potential to capture the spatial pattern of soil $\delta^{13}\text{C}$ (Figure 4). The modelled soil $\delta^{13}\text{C}$ showed great spatial variation across the TP, with the highest soil $\delta^{13}\text{C}$ values observed in the western region and the lowest values found in Southeastern region and Tsaidam Basin (Figure 5). Across the TP, soil $\delta^{13}\text{C}$ ranged from -32% to -15.46% , with a mean value of -23.35% .

Predicted β showed strong spatial variabilities across the TP (Figure 6). The highest β values were found in middle east region with β values close to 0, while the lowest values were observed in the southern TP and Tsaidam Basin, with β lower than -3 . Mean β was -1.81 across the TP.

4. Discussion

4.1. Soil $\delta^{13}\text{C}$ across Ecosystem Types

Significant differences in topsoil $\delta^{13}\text{C}$ were observed across ecosystems, with an increasing trend from forests (-25.2%) to shrublands (-24.4%), grasslands (-23.3%), and deserts (-23%) (Table S1). This result is in line with a previous study, which found a topsoil $\delta^{13}\text{C}$ ($0 \sim 10$ cm) of -25.25% for forests, -24.71% for meadows, and -23.65% for steppes (Wang et al., 2012). These differences were primarily due to the climate variations from southeast to northwest of the TP, which were important variables controlling soil $\delta^{13}\text{C}$ and vegetation distribution and water use efficiency (more details in discussion 4.2). Besides, topsoil $\delta^{13}\text{C}$ varied greatly was shown within the same ecosystem, such as grasslands and desert, which was associated to the wide distribution of observations within the same vegetation type across the TP. Meanwhile, the original observational data categorized vegetation types into four major classes, and this study did not further divide them sub-ecosystem types (Figure 1). The importance analysis results had indicated that soil moisture and precipitation were the most important environmental factors (Figure 3). However, there were obvious differences in climate, vegetation, and soil environmental factors among same ecosystem from southeast to northwest of the TP, resulting in large variations soil $\delta^{13}\text{C}$ within the same ecological type.

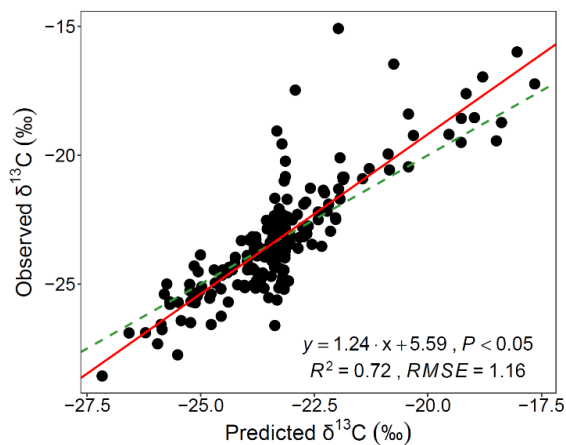


Figure 4. Correlations between observed and predicted soil $\delta^{13}\text{C}$ from MLP by 10-fold cross-validation. The green line represents the 1:1 line.

4.2. Spatial Variation of Soil $\delta^{13}\text{C}$ across the TP

We found a great spatial pattern in soil $\delta^{13}\text{C}$, with an increasing trend from the southeastern to the northwestern TP. Such spatial patterns may be primarily associated with vegetation types (Wang et al., 2012), because we found that vegetation type was the most important factor in predicting soil $\delta^{13}\text{C}$ (Figure S2). Plant litter was the primary source of soil organic matter, exhibiting significant variation across ecosystem types. Therefore, the substantial variations in leaf $\delta^{13}\text{C}$ among distinct vegetation types can exert a noteworthy influence on soil $\delta^{13}\text{C}$ (Wang et al., 2012; Yang et al., 2015). Plant species growing in dry habitats generally have higher leaf $\delta^{13}\text{C}$ values (Wang et al., 2012). For example, in the high-altitude regions of the Tibetan Plateau, C_4 plants, which initially synthesize compounds containing four carbon atoms (such as malic acid or aspartate) when absorbing carbon dioxide from the air, exhibiting remarkable resilience to severe drought conditions. These C_4 plants display significantly higher leaf $\delta^{13}\text{C}$ values in comparison to C_3 plants, which utilize a different photosynthetic pathway involving the three-carbon compound 3-phosphoglyceric acid (Wang et al., 2004). Meanwhile, the degree of carbon isotope fractionation during the conversion of soil organic matter from different regions and plant residues varied, ranging from 0.5% to 2% (Cao et al., 2005). The southeastern TP is predominantly characterized by forests, whereas the northwestern TP is mainly composed of deserts and grasslands (Wang et al., 2012). Consequently, this stark contrast could potentially result in higher soil $\delta^{13}\text{C}$ in the northwestern TP, while the southeastern TP may exhibit lower soil $\delta^{13}\text{C}$ (Figure 4). Therefore, through the measurement of carbon isotope ratios across different vegetation types, we were able to accurately quantify and compare the distribution patterns and sources of carbon among different types of vegetation.

Besides vegetation types, climate factors also played a crucial role in influencing the spatial variation of soil $\delta^{13}\text{C}$ (Rao et al., 2012; Wang et al., 2013; Zhao et al., 2017). Our results revealed a notable negative correlation between soil $\delta^{13}\text{C}$ and temperature (Figure 3), indicating that temperature can exert a significant influence on soil $\delta^{13}\text{C}$. These results align with Rao et al. (2017) and Zhang et al. (2020), which similarly reported a decrease in soil $\delta^{13}\text{C}$ with increasing temperature. However, our results diverged from those reported by Wang et al. (2012) and Brunn et al. (2014), who observed a positive correlation between soil $\delta^{13}\text{C}$ and temperature. This contrasting results suggest that the relationship between temperature and soil $\delta^{13}\text{C}$ is complex (Rao et al., 2017). First, the temperature can affect soil $\delta^{13}\text{C}$ by changing vegetation and microbial $\delta^{13}\text{C}$. For example, temperature can affect the relative abundance of C_3 and C_4 plants (Tieszen et al., 1997). Generally, a relatively higher abundance of C_4 plants distribution is found in areas with high temperature and low precipitation (Zhang et al., 2003). Second, temperature can also affect carbon isotope by modulating the water-use efficiency in plants (Zhao et al., 2017). Increasing temperature increases leaf transpiration (Moore et al., 2021), which can potentially cause water deficit in plants (Wu et al., 2018). Water deficits, may lower either stomatal conductance or stomatal density in the dry TP, resulting in higher water-use efficiency and positive

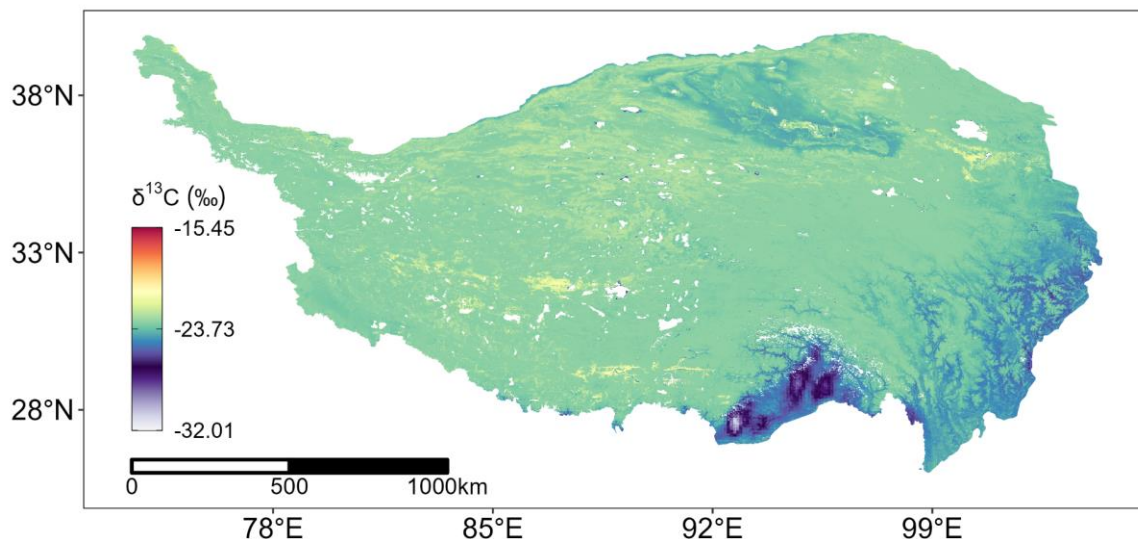


Figure 5. Spatial distributions of soil $\delta^{13}\text{C}$ across the Tibetan Plateau.

leaf $\delta^{13}\text{C}$ values in plants (Song et al., 2021; Laffitte et al., 2022). Third, temperature could also affect soil $\delta^{13}\text{C}$ by regulating litter decomposition rate and ecosystem respiration. Generally, high temperature lead to high litter decomposition and ecosystem respiration (Kato et al., 2004; Cai et al., 2021), resulting in enriched soil $\delta^{13}\text{C}$. Fourth, temperature can also affect soil $\delta^{13}\text{C}$ by changing the isotopic fractionation during the microbial decomposition (Garten, 2006). Based on the microbial substrate utilizing preference hypothesis (Natlhoffer et al., 1988), microbes tend to use lighter ^{12}C during decomposition. Most of the lighter ^{12}C is emitted into the atmosphere through microbial respiration (Qu et al., 2022), and microbial residues contribute significantly, accounting for 45.5% of SOC in grasslands (He et al., 2021). This contribution enriches soil ^{13}C . Consequently, the relationships between soil $\delta^{13}\text{C}$ and temperature can be attributed to changes in vegetation composition, vegetation water-use efficiency, ecosystem respiration, and litter decomposition with its microbial characteristics.

Precipitation is another important factor influencing soil $\delta^{13}\text{C}$ and soil $\delta^{13}\text{C}$ decreases with increasing precipitation (Figure 3). This finding is consistent with previous studies (Murphy et al., 2009; Zhao et al., 2019). The mechanisms of the impact of precipitation on soil $\delta^{13}\text{C}$ have been well elucidated. First, when water is scarce, plants close their stomata to conserve water, a process known as reduced transpiration (Farquhar et al., 1989), leading to an increase in soil $\delta^{13}\text{C}$. Second, the TP has undergone a significant increase in precipitation over the past several decades. This increases likely enhanced microbial biodiversity, quantity, and activity (Papatheodorou et al., 2004), resulting in an accelerated decomposition rate of ^{12}C to a certain degree, and an enrichment of soil $\delta^{13}\text{C}$ (Li et al., 2020). However, it should be noted that although precipitation increased in the TP, some regions still suffered from a lack of precipitation, particularly in its northwestern part. Therefore, the northwestern TP exhibited higher soil $\delta^{13}\text{C}$ compared to other regions within the TP (Figure 4).

Soil factors also importantly control soil $\delta^{13}\text{C}$ by altering plant type, microbial activity, matrix quality, and effectiveness, particularly in the TP cold and dry area (Wynn et al., 2006; Xu et al., 2016; Zhou et al., 2022). In this study, we found a negative correlation between soil $\delta^{13}\text{C}$ and SOC (Figure S1), which is consistent with previous studies (Yang et al., 2015; Wang et al., 2018). Volk et al. (2018) Proposed that the preferential substrate use of $\delta^{12}\text{C}$ and the kinetic fractionation of the heavier ^{13}C during decomposition processes contribute to the emergence of this phenomenon. Previous studies have also indicated that soil texture could affect soil $\delta^{13}\text{C}$. This could be attributed to the reduction in particle size associated with soil texture, which leads to the allocation of carbon enriched in soil $\delta^{13}\text{C}$ to microbial biomass. Subsequently, this carbon can be stabilized through interactions with fine mineral phases in the soil (Sollins et al., 2009; Kleber et al., 2011). However, we did not find significant correlations between soil $\delta^{13}\text{C}$ and soil texture (Figure 3). Such finding may be attributed to potential discrepancies between the datasets used and the spatial mismatch between observations and the extracted environmental variables, which were obtained at a spatial resolution of 500 m (see method section). Specially, the soil silt was found to be less important compared to other variables due to fast change in climate variables in the TP, while the soil texture remained more stable in a short term (Yang et al., 2017). Notably, the TP is known to face relatively serious phosphorus limitation (Li et al., 2022). Hence, the combination of higher temperatures and insufficient precipitation increases the demand for rhizosphere microorganisms in transforming organic matter to obtain nutrients, thereby intensifying soil processes (Zheng et al., 2022). Therefore, the large variability of topsoil $\delta^{13}\text{C}$ across the TP was closely associated to vegetation type, climate and soil, which has an important implication to SOC dynamics and highlighted complex environmental controls on SOC. These complex processes should be further incorporated the biogeochemical models to modeling regional or global SOC dynamics because the majority of the interaction effects of soil, vegetation and climate on SOC dynamics are largely simplified.

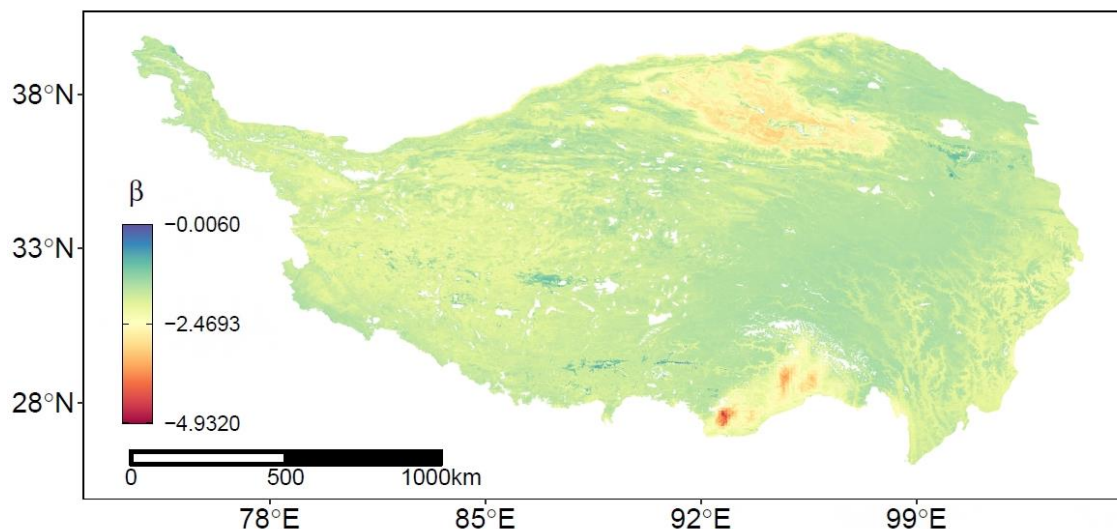


Figure 6. Spatial distributions of soil β across the TP.

4.3. Spatial Pattern of β

Soil carbon turnover is a major determinant of the capacity of soil carbon sequestration (Luo et al., 2003), and a decrease in carbon turnover can sequester SOC without an increase in carbon input (Jastrow et al., 2006). Because it is difficult to detect changes in SOC stocks over short periods due to the large pool size and huge spatial heterogeneity (Van Groenigen et al., 2014), the predicted β across the TP could provide a reliable method to evaluate the SOC turnover rate over a large spatial scale (Brunn, et al., 2014; Gautam et al., 2017). Therefore, understanding the spatial variation of the β values is particularly important.

The β values reflect the turnover rate of SOC in response to microbial activities. The more negative the β values, the faster the turnover of SOC (Acton et al., 2013; Zhao et al., 2019). The average β value in our study was -1.81 , which lied the range of -1.77 to -2.87 (mean value of -2.31) from field observations across the TP reported by (Li et al., 2020). Numerous studies have compared β values across different ecosystem types throughout the TP and have proposed that β serves as a valuable proxy for comprehending generalized patterns of SOC turnover and the underlying factors governing soil metabolism (Wang et al., 2018). The predicted β showed a substantial spatial variability across the TP, indicating a pronounced variation in soil carbon turnover. This variability can be attributed to climatic variables, with temperature and precipitation being key factors influencing SOC turnover (Wang et al., 2017; Li, et al., 2020). Generally, higher temperatures and precipitation have a positive impact on vegetation development, resulting in an augmentation of biological sources of SOC (Kögel-Knabner, 2017; Deng et al., 2022). Additionally, these climatic conditions enhance microbial biomass and enzyme activity (Conant et al., 2011), further contributing to SOC dynamics. The lowest β values, below -4 , were observed in the southern TP, suggesting a faster SOC turnover compared to other regions of the TP. This finding may be related with the higher abundance of precipitation and elevated tem-

peratures in the southern TP (Figures S3 and S4), which are known to significantly enhance microbial activities involved in SOC decomposition (Collins et al., 2008). Our result is consistent with a previous study that demonstrated an increase in SOC turnover that SOC turnover with rising temperature and precipitation on a global scale (Wang et al., 2018).

In addition to climate, soil properties played a significant role in determining SOC turnover. A previous study indicated that β values were generally negatively correlated with sand content and positively correlated with clay content in the TP (Li et al., 2020). Our results are in line with this study. Specifically, we found higher β values in the northwestern TP, characterized by low soil sand content and high soil clay content (Figures S5 and S6). Soil texture properties have well-established effects on SOC turnover by influencing soil water-holding capacity, water movement, and gas diffusion (Luo et al., 2006; Kaiser et al., 2015; Xu et al., 2016). Meanwhile, soil pH can also influence SOC turnover through its impact on microbial community, enzyme activity, and substrate availability (Priha et al., 2001). Therefore, understanding the dominant environmental factors driving β values can enhanced our ability to predict spatial patterns of SOC turnover and provided insights into the potential response of SOC to future climate changes.

4.4. Limitations

In this study, we employed a modified MLP model method to predict the spatial patterns of topsoil $\delta^{13}\text{C}$ and β in the TP, based on field observations. However, we noted several limitations to consider. First, the MLP algorithm builds a model based on the training dataset, which is often limited by data in terms of quantity, quality, and representativeness. Uneven data distribution has long been recognized as a significant issue in numerous ecological studies worldwide, e.g., Jung et al. (2011) and Xu et al. (2016). The field observations of topsoil $\delta^{13}\text{C}$ were mainly concentrated in the eastern and northern TP, while there

was a lack of topsoil $\delta^{13}\text{C}$ field observations in the western and northwestern TP. Therefore, the uneven coverage of observations was an important source of uncertainty in predicting topsoil $\delta^{13}\text{C}$, which could cause biases in the MLP model towards the areas with more observations. Enhancing the number of field observations in the eastern and northern TP could improve the capability to assess the spatial patterns of topsoil $\delta^{13}\text{C}$ across the TP. Second, our dataset was limited to the topsoil within the range of 0 ~ 3 cm, which constrained the model availability in topsoil, while it could not capture carbon sequestration capability in subsoil. It is widely accepted that the topsoil contains higher carbon content and exhibits greater sensitivity to environmental changes compared to subsoils. Therefore, modeling approaches for deeper soils would enhance our understanding of soil carbon dynamics and provide valuable insights into the response of soil carbon to subsoils. Third, focusing on topsoil is another limitation in current study. Luo et al. (2019) indicated that subsoil SOC storage was twice that of the topsoil. Therefore, further studies focus on subsoil should be conducted to order to have a comprehensive understanding of subsoil SOC dynamics and turnover time.

5. Conclusions

In this study, we employed modified MLP model to predict the spatial patterns and the drivers of topsoil $\delta^{13}\text{C}$ and β at a high spatial resolution of 500 m in the TP based on field observations and environmental factors, including vegetation, climate, and soil. Key findings revealed spatial heterogeneity, with notable differences between the southeastern and northwestern regions in terms of topsoil $\delta^{13}\text{C}$ and β . Higher turnover rates of SOC accelerated the carbon cycling process and reduced the abundance of topsoil $\delta^{13}\text{C}$. Meanwhile, vegetation played a crucial role in influencing carbon cycling, with temperature and precipitation emerging as important drivers. In addition, we found that the MLP model, based on 10-fold cross validation, demonstrated its ability to extrapolate data from a point scale to a regional or global scale, providing a feasible approach for understanding carbon cycling processes in the TP amidst ongoing climate change. In conclusion, these findings contribute to a broader understanding of the dynamics of the carbon cycle in the TP and have practical implications for assessing the impact of climate change on SOC distribution and sequestration in this ecologically significant region.

Acknowledgements. This study was primarily supported by the National Natural Science Fund Program (32271856), Everest Scientific Research Program, Chengdu University of Technology (80000-2023-ZF11410), Sichuan Science and Technology Program (2019YFG0460, 2021YJ0377), State Key Laboratory of Geohazard Prevention and Geoenvironment Protection Independent Research Project (SKLGP2018Z004, SKLGP2021K024), Large-Scale Engineering Projects of Hunneng, China (JC2022/D01). The authors express their great thanks to the contributors of the dataset used in this study. Great thanks were also given to Benjamin Laffitte for his insightful language improvement.

References

- Acton, P., Fox, J., Campbell, E., Rowe, H. and Wilkinson, M. (2013). Carbon isotopes for estimating soil decomposition and physical mixing in well-drained forest soils. *J. Geophys. Res. Biogeosci.*, 118(4), 1532-1545. <https://doi.org/10.1002/2013JG002400>
- Averill, C., Turner, B.L. and Finzi, A.C. (2014). Mycorrhiza-mediated competition between plants and decomposers drives soil carbon storage. *Nature*, 505(7484), 543-545. <https://doi.org/10.1038/nature12901>
- Bateni, S.M., Emamgholizadeh, S. and Shahsavani, D. (2014). Estimating soil cation exchange capacity from soil physical and chemical properties. *AGU Fall Meeting Abstracts*.
- Blagodatskaya, E., Yuyukina, T., Blagodatsky, S. and Kuzyakov, Y. (2011). Turnover of soil organic matter and of microbial biomass under C-3-C-4 vegetation change: Consideration of C-13 fractionation and preferential substrate utilization. *Soil Biol. Biochem.*, 43(1), 159-166. <https://doi.org/10.1016/j.soilbio.2010.09.028>
- Bodesheim, P., Jung, M., Gans, F., Mahecha, M.D. and Reichstein, M. (2018). Upscaled diurnal cycles of land-atmosphere fluxes: a new global half-hourly data product. *Earth Syst. Sci. Data*, 10(3), 1327-1365. <https://doi.org/10.5194/essd-10-1327-2018>
- Bogino, S.M. and Bravo, F. (2014). Carbon stable isotope-climate association in tree rings of *Pinus pinaster* and *Pinus sylvestris* in Mediterranean environments. *Bosque*, 35(2), 175-184. <http://dx.doi.org/10.4067/S0717-92002014000200005>
- Bretz, F., Hothorn, T. and Westfall, P. (2010). *Multiple Comparisons Using R*. Chapman & Hall/CRC. <https://doi.org/10.1201/9781420010909>
- Brunn, M., Spielvogel, S., Sauer, T. and Oelmann, Y. (2014). Temperature and precipitation effects on delta $\delta^{13}\text{C}$ depth profiles in SOM under temperate beech forests. *Geoderma*, 235, 146-153. <https://doi.org/10.1016/j.geoderma.2014.07.007>
- Cai, A.D., Liang, G.P., Yang, W., Zhu, J., Han, T.F., Zhang, W.J. and Xu, M.G. (2021). Patterns and driving factors of litter decomposition across Chinese terrestrial ecosystems. *J. Clean. Prod.*, 278, 9. <https://doi.org/10.1016/j.jclepro.2020.123964>
- Campbell, J.E., Fox, J.F., Davis, C.M., Rowe, H.D. and Thompson, N. (2009). Carbon and Nitrogen Isotopic Measurements from Southern Appalachian Soils: Assessing Soil Carbon Sequestration under Climate and Land-Use Variation. *J. Environ. Eng.*, 135(6), 439-448. [https://doi.org/10.1061/\(ASCE\)EE.1943-7870.0000008](https://doi.org/10.1061/(ASCE)EE.1943-7870.0000008)
- Cao, Y., Liu, W., Ning, Y., Zhang, Q. and Wang, Z. (2005). Effects of soil sample preparation process on $\delta^{13}\text{C}$ of organic matter. *Geochemistry*, 34(4), 395-403. <https://link.cnki.net/doi/10.19700/j.0379-1726.2005.04.012>
- Carvalho, D.C.d., Pereira, M.G., Guareschi, R.F., Simon, C.A., Toledo, L.d.O. and Piccolo, M.d.C. (2017). Carbon, Nitrogen and Natural Abundance of $\delta^{13}\text{C}$ in Forest Cover. *Floresta e Ambiente*, 24, e20150093-e20150093. <https://doi.org/10.1590/2179-8087.009315>
- Chang, X., Wang, S., Luo, C., Zhang, Z., Duan, J., Zhu, X., Lin, Q. and Xu, B. (2012). Responses of soil microbial respiration to thermal stress in alpine steppe on the Tibetan plateau. *Eur. Soil Sci.*, 63(3), 325-331. <https://doi.org/10.1111/j.1365-2389.2012.01441.x>
- Collins, S.L., Sinsabaugh, R.L., Crenshaw, C., Green, L., Porras-Alfaro, A., Stursova, M. and Zeglin, L.H. (2008). Pulse dynamics and microbial processes in aridland ecosystems. *J. Ecol.*, 96(3), 413-420. <https://doi.org/10.1111/j.1365-2745.2008.01362.x>
- Conant, R.T., Ryan, M.G., Agren, G.I., Birge, H.E., Davidson, E.A., Eliasson, P.E., Evans, S.E., Frey, S.D., Giardina, C.P., Hopkins, F.M., Hyvonen, R., Kirschbaum, M.U.F., Lavallee, J.M., Leifeld, J., Parton, W.J., Steinweg, J.M., Wallenstein, M.D., Wetterstedt, J.A.M. and Bradford, M.A. (2011). Temperature and soil organic matter decomposition rates - synthesis of current knowledge and a way forward. *Glob. Change Biol.*, 17(11), 3392-3404. <https://doi.org/10.1111/j.1365-2486.2011.02496.x>

- Deng, F. and Liang, C. (2022). Revisiting the quantitative contribution of microbial necromass to soil carbon pool: Stoichiometric control by microbes and soil. *Soil Biol. Biochem.*, 165, 108486. <https://doi.org/10.1016/j.soilbio.2021.108486>
- Didan, K. (2021). MODIS/Terra Vegetation Indices 16-Day L3 Global 250m SIN Grid V061 [Dataset]. *NASA EOSDIS Land Processes Distributed Active Archive Center*. <https://doi.org/10.5067/MODIS/MOD13Q1.061>
- Dong, S., Li, Y., Zhao, Z., Li, Y., Liu, S., Zhou, H., Dong, Q., Li, S., Gao, X., Shen, H., Xu, Y., Han, Y., Zhang, J. and Yang, M. (2018). Land Degradation Enriches Soil $\delta^{13}\text{C}$ in Alpine Steppe and Soil $\delta^{15}\text{N}$ in Alpine Desert by Changing Plant and Soil Features on Qinghai-Tibetan Plateau. *Soil Sci. Soc. Am. J.*, 82(4), 960-968. <https://doi.org/10.2136/sssaj2018.01.0017>
- Duan, A.M. and Xiao, Z.X. (2015). Does the climate warming hiatus exist over the Tibetan Plateau? *Sci. Rep.*, 5, 13711. <https://doi.org/10.1038/srep13711>
- Ehleringer, J.R., Buchmann, N. and Flanagan, L.B. (2000). Carbon isotope ratios in belowground carbon cycle processes. *Ecol. Appl.*, 10(2), 412-422. [https://doi.org/10.1890/1051-0761\(2000\)010\[0412:CIRIBC\]2.0.CO;2](https://doi.org/10.1890/1051-0761(2000)010[0412:CIRIBC]2.0.CO;2)
- Fan, X., Gao, D., Zhao, C., Wang, C., Qu, Y., Zhang, J. and Bai, E. (2021). Improved model simulation of soil carbon cycling by representing the microbially derived organic carbon pool. *ISME J.*, 15(8), 2248-2263. <https://doi.org/10.1038/s41396-021-00914-0>
- Fang, J., Yang, Y., Ma, W., Mohammat, A. and Shen, H. (2010). Ecosystem carbon stocks and their changes in China's grasslands. *Sci. China Life Sci.*, 53(7), 757-765. <https://doi.org/10.1007/s11427-010-4029-x>
- Farquhar, G.D., Ehleringer, J.R. and Hubick, K.T. (1989). Carbon isotope discrimination and photosynthesis. *Annu. Rev. Plant Biol.*, 40(1), 503-537. <https://doi.org/10.1146/annurev.pp.40.060189.002443>
- Friedl, M., and Sulla-Menashe, D. (2022). MODIS/Terra + Aqua Land Cover Type Yearly L3 Global 500m SIN Grid V061 [Dataset]. *NASA EOSDIS Land Processes DAAC: Sioux Falls, SD, USA*. <https://doi.org/10.5067/MODIS/MCD12Q1.061>
- Garten, C.T. (2006). Relationships among forest soil C isotopic composition, partitioning, and turnover times. *Can. J. For. Res.*, 36(9), 2157-2167. <https://doi.org/10.1139/x06-115>
- Garten, C.T., Cooper, L.W., Post, W.M. and Hanson, P.J. (2000). Climate controls on forest soil C isotope ratios in the Southern Appalachian Mountains. *Ecology*, 81(4), 1108-1119. <https://doi.org/10.2307/177182>
- Garten, C.T. and Hanson, P.J. (2006). Measured forest soil C stocks and estimated turnover times along an elevation gradient. *Geoderma*, 136(1-2), 342-352. <https://doi.org/10.1016/j.geoderma.2006.03.049>
- Gautam, M.K., Lee, K.S., Song, B.Y. and Bong, Y.S. (2017). Site related delta C-13 of vegetation and soil organic carbon in a cool temperate region. *Plant and Soil*, 418(1-2), 293-306. <https://doi.org/10.1007/s11104-017-3284-z>
- Gomez-Fernandez, M., Wong, W.-K., Tokuhiko, A., Welter, K., Alhawsawi, A.M., Yang, H. and Higley, K.J.N.I. (2021). Isotope identification using deep learning: An explanation. *Nuclear Instruments and Methods in Physics Research Section A: Accelerators, Spectrometers, Detectors and Associated Equipment*, 988, 164925. <https://doi.org/10.1016/j.nima.2020.164925>
- Gorelick, N., Hancher, M., Dixon, M., Ilyushchenko, S., Thau, D. and Moore, R. (2017). Google Earth Engine: Planetary-scale geospatial analysis for everyone. *Remote Sens. Environ.*, 202, 18-27. <https://doi.org/10.1016/j.rse.2017.06.031>
- He, M., Fang, K., Chen, L., Feng, X., Qin, S., Kou, D., He, H., Liang, C. and Yang, Y. (2021). Depth - dependent drivers of soil microbial necromass carbon across Tibetan alpine grasslands. *Glob. Change Biol.*, 28, 936-949. <https://doi.org/10.1111/gcb.15969>
- Hengl, T. and Gupta, S. (2019). Soil water content (volumetric %) for 33kPa and 1500kPa suctions predicted at 6 standard depths (0, 10, 30, 60, 100 and 200 cm) at 250 m resolution (v0.1) [Dataset]. *Zenodo*. <https://doi.org/10.5281/zenodo.2784001>
- Hengl, T., Mendes de Jesus, J., Heuvelink, G.B., Ruiperez Gonzalez, M., Kilibarda, M., Blagotic, A., Shangguan, W., Wright, M.N., Geng, X., Bauer-Marschallinger, B., Guevara, M.A., Vargas, R., MacMillan, R.A., Batjes, N.H., Leenaars, J.G., Ribeiro, E., Wheeler, I., Mantel, S. and Kempen, B. (2017). SoilGrids250m: Global gridded soil information based on machine learning. *PLoS One*, 12(2), e0169748. <http://doi.org/10.1371/journal.pone.0169748>
- Jaber, S.M., Lant, C.L. and Al-Qinna, M.I. (2011). Estimating spatial variations in soil organic carbon using satellite hyperspectral data and map algebra. *Int. J. Remote Sens.*, 32(18), 5077-5103. <https://doi.org/10.1080/01431161.2010.494637>
- Jastrow, J.D., Amonette, J.E. and Bailey, V.L. (2006). Mechanisms controlling soil carbon turnover and their potential application for enhancing carbon sequestration. *Climatic Change*, 80(1-2), 5-23. <https://doi.org/10.1007/s10584-006-9178-3>
- Jian, J.S., Steele, M.K., Thomas, R.Q., Day, S.D. and Hodges, S.C. (2018). Constraining estimates of global soil respiration by quantifying sources of variability. *Glob. Change Biol.*, 24(9), 4143-4159. <https://doi.org/10.1111/gcb.14301>
- Jin, Y.Q. and Liu, C. (1997). Biomass retrieval from high-dimensional active/passive remote sensing data by using artificial neural networks. *Int. J. Remote Sens.*, 18(4), 971-979. <https://doi.org/10.1080/014311697218863>
- Julian Martinon-Martinez, R., Jesus Vargas-Hernandez, J., Gomez-Guerrero, A. and Lopez-Upton, J. (2011). Carbon isotopic composition in foliage of *Pinus pinceana* Gordon seedlings subjected to water and temperature stress. *Agrociencia*, 45(2), 245-258. <https://api.semanticscholar.org/CorpusID:82498732>
- Jung, M., Reichstein, M., Margolis, H.A., Cescatti, A., Richardson, A.D., Arain, M.A., Arneth, A., Bernhofer, C., Bonal, D., Chen, J.Q., Gianelle, D., Gobron, N., Kiely, G., Kutsch, W., Lasslop, G., Law, B.E., Lindroth, A., Merbold, L., Montagnani, L., Moors, E.J., Papale, D., Sottocornola, M., Vaccari, F. and Williams, C. (2011). Global patterns of land-atmosphere fluxes of carbon dioxide, latent heat, and sensible heat derived from eddy covariance, satellite, and meteorological observations. *J. Geophys. Res. Biogeosci.*, 116, 16. <https://doi.org/10.1029/2010jg001566>
- Kaiser, M., Kleber, M. and Berhe, A.A. (2015). How air-drying and rewetting modify soil organic matter characteristics: An assessment to improve data interpretation and inference. *Soil Biol. Biochem.*, 80, 324-340. <https://doi.org/10.1016/j.soilbio.2014.10.018>
- Kato, T., Tang, Y.H., Gu, S., Cui, X.Y., Hirota, M., Du, M.Y., Li, Y.N., Zhao, Z.Q. and Oikawa, T. (2004). Carbon dioxide exchange between the atmosphere and an alpine meadow ecosystem on the Qinghai-Tibetan Plateau, China. *Agric. For. Meteorol.*, 124(1-2), 121-134. <https://doi.org/10.1016/j.agrformet.2003.12.008>
- Khan, K.S., Gattinger, A., Buegger, F., Schloter, M. and Joergensen, R.G. (2008). Microbial use of organic amendments in saline soils monitored by changes in the C-13/C-12 ratio. *Soil Biol. Biochem.*, 40(5), 1217-1224. <https://doi.org/10.1016/j.soilbio.2007.12.016>
- Kleber, M., Nico, P.S., Plante, A., Filley, T., Kramer, M., Swanston, C. and Sollins, P. (2011). Old and stable soil organic matter is not necessarily chemically recalcitrant: implications for modeling concepts and temperature sensitivity. *Glob. Change Biol.*, 17(2), 1097-1107. <https://doi.org/10.1111/j.1365-2486.2010.02278.x>
- Köchy, M., Hiederer, R. and Freibauer, A. (2015). Global distribution of soil organic carbon - Part 1: Masses and frequency distributions of SOC stocks for the tropics, permafrost regions, wetlands, and the world. *Soil*, 1(1), 351-365. <http://doi.org/10.5194/soil-1-351-2015>
- Kögel-Knabner, I. (2017). The macromolecular organic composition of plant and microbial residues as inputs to soil organic matter: Fourteen years on. *Soil Biol. Biochem.*, 105, A3-A8. <https://doi.org/10.1016/j.soilbio.2016.08.011>
- Kuang, B., Tekin, Y. and Mouazen, A.M. (2015). Comparison between

- artificial neural network and partial least squares for on-line visible and near infrared spectroscopy measurement of soil organic carbon, pH and clay content. *Soil Tillage Res.*, 146, 243-252. <https://doi.org/10.1016/j.still.2014.11.002>
- Laffitte, B., Seyler, B.C., Wang, W., Li, P., Du, J. and Tang, Y. (2022). Declining tree growth rates despite increasing water-use efficiency under elevated CO₂ reveals a possible global overestimation of CO₂ fertilization effect. *Heliyon*, 8(10), e11219. <https://doi.org/10.1016/j.heliyon.2022.e11219>
- Lawrence, D.M., Fisher, R.A., Koven, C.D., Oleson, K.W., Swenson, S.C., Bonan, G., Collier, N., Ghimire, B., van Kampenhou, L. and Kennedy, D. (2019). The Community Land Model version 5: Description of new features, benchmarking, and impact of forcing uncertainty. *J. Adv. Model. Earth Syst.*, 11(12), 4245-4287. <https://doi.org/10.1029/2018MS001583>
- LeCun, Y., Bengio, Y. and Hinton, G. (2015). Deep learning. *Nature*, 521(7553), 436-444. <https://doi.org/10.1038/nature14539>
- Li, H., Yan, F., Tuo, D., Yao, B. and Chen, J. (2020). The effect of climatic and edaphic factors on soil organic carbon turnover in hummocks based on delta(13)C on the Qinghai-Tibet Plateau. *Sci. Total Environ.*, 741, 140141. <https://doi.org/10.1016/j.scitotenv.2020.140141>
- Li, M., Hai, X., Hong, H., Shao, Y., Peng, D., Xu, W., Yang, Y., Zheng, Y. and Xia, Z. (2019). Modelling soil detachment by overland flow for the soil in the Tibet Plateau of China. *Sci. Rep.*, 9(1), 8063. <https://doi.org/10.1038/s41598-019-44586-5>
- Li, Y., Huang, Y., Ji, D., Cheng, Y., Nwankwegu, A., Paerl, H., Tang, C., Yang, Z., Zhao, X., Chen, Y. and Li, J. (2022). Storm and floods increase the duration and extent of phosphorus limitation on algal blooms in a tributary of the Three Gorges Reservoir, China. *J. Hydrol.*, 607, 127562. <https://doi.org/10.1016/j.jhydrol.2022.127562>
- Liang, J., Xia, J., Shi, Z., Jiang, L., Ma, S., Lu, X., Mauritz, M., Natali, S.M., Pegoraro, E. and Penton, C.R. (2018). Biotic responses buffer warming-induced soil organic carbon loss in Arctic tundra. *Glob. Change Biol.*, 24(10), 4946-4959. <https://doi.org/10.1111/gcb.14325>
- Lipovetsky, S. (2022). Explanatory Model Analysis: Explore, Explain and Examine Predictive Models. *Technometrics*, 64(3), 423-424. <https://doi.org/10.1080/00401706.2022.2091871>
- Liu, W., Lü, H.H., Chen, Y.X. and Wu, W.X. (2008). Application of stable carbon isotope technique in the research of carbon cycling in soil-plant system. *Ying Yong Sheng Tai Xue Bao*, 19(3), 674-680. <https://www.cjae.net/CN/Y2008/V19/I03/674>
- Lu, H.Y., Wu, N.Q., Gu, Z.Y., Guo, Z.T., Wang, L., Wu, H.B., Wang, G., Zhou, L.P., Han, J.M. and Liu, T.S. (2004). Distribution of carbon isotope composition of modern soils on the Qinghai-Tibetan Plateau. *Biogeochemistry*, 70(2), 273-297. <https://doi.org/10.1023/B:BI0G.0000049343.48087.ac>
- Luo, Y. and Zhou, X. (2006). Preface. Soil Respiration and the Environment. In *Luo and Zhou (Eds.)*. Burlington: Academic Press, pp ix-xi. <https://doi.org/10.1016/B978-0-12-088782-8.X5000-1>
- Luo, Y.Q., White, L.W., Canadell, J.G., DeLucia, E.H., Ellsworth, D.S., Finzi, A.C., Lichten, J. and Schlesinger, W.H. (2003). Sustainability of terrestrial carbon sequestration: A case study in Duke Forest with inversion approach. *Global Biogeochem. Cy.*, 17(1), 13. <https://doi.org/10.1029/2002GB001923>
- Luo, Z., Wang, G. and Wang, E. (2019). Global subsoil organic carbon turnover times dominantly controlled by soil properties rather than climate. *Nat. Commun.*, 10(1), 3688. <https://doi.org/10.1038/s41467-019-11597-9>
- Mattei, F. and Scardi, M. (2020). Embedding ecological knowledge into artificial neural network training: A marine phytoplankton primary production model case study. *Ecol. Modell.*, 421, 1. <https://doi.org/10.1016/j.ecolmodel.2020.108985>
- Moore, C.E., Meacham-Hensold, K., Lemonnier, P., Slattery, R.A., Benjamin, C., Bernacchi, C.J., Lawson, T. and Cavanagh, A.P. (2021). The effect of increasing temperature on crop photosynthesis: from enzymes to ecosystems. *J. Exp. Bot.*, 72(8), 2822-2844. <https://doi.org/10.1093/jxb/erab090>
- Muñoz Sabater, J. (2019). ERA5-Land Hourly Data from 1981 to Present. Copernicus Climate Change Service (C3S) Climate Data Store (CDS). <https://doi.org/10.24381/cds.68d2bb30>
- Murphy, B.P. and Bowman, D.M.J.S. (2009). The carbon and nitrogen isotope composition of Australian grasses in relation to climate. *Funct. Ecol.*, 23(6), 1040-1049. <https://doi.org/10.1111/j.1365-2435.2009.01576.x>
- Myneni, R., Knyazikhin, Y., and Park, T. (2021). MODIS/Terra Leaf Area Index/FPAR 8-Day L4 Global 500m SIN Grid V061 [Dataset]. NASA EOSDIS Land Processes DAAC. <https://doi.org/10.5067/MODIS/MOD15A2H.061>
- Natelloffer, K. and Fry, B. (1988). Controls on natural nitrogen-15 and carbon-13 abundances in forest soil organic matter. *Soil Sci. Soc. Am. J.*, 52(6), 1633-1640. <https://doi.org/10.2136/sssaj1988.03615995005200060024x>
- Papathodorou, E.M., Argyropoulou, M.D. and Stamou, G.P. (2004). The effects of large- and small-scale differences in soil temperature and moisture on bacterial functional diversity and the community of bacterivorous nematodes. *Appl. Soil Ecol.*, 25(1), 37-49. [https://doi.org/10.1016/S0929-1393\(03\)00100-8](https://doi.org/10.1016/S0929-1393(03)00100-8)
- Parton, W.J., Schimel, D.S., Cole, C.V. and Ojima, D.S. (1987). Analysis of factors controlling soil organic matter levels in Great Plains grasslands. *Soil Sci. Soc. Am. J.*, 51(5), 1173-1179. <https://doi.org/10.2136/sssaj1987.03615995005100050015x>
- Peri, P.L., Ladd, B., Pepper, D.A., Bonser, S.P., Laffan, S.W. and Amelung, W. (2012). Carbon ($\delta^{13}C$) and nitrogen ($\delta^{15}N$) stable isotope composition in plant and soil in Southern Patagonia's native forests. *Glob. Change Biol.*, 18(1), 311-321. <https://doi.org/10.1111/j.1365-2486.2011.02494.x>
- Priha, O., Grayston, S.J., Hiukka, R., Pennanen, T. and Smolander, A. (2001). Microbial community structure and characteristics of the organic matter in soils under *Pinus sylvestris*, *Picea abies* and *Betula pendula* at two forest sites. *Biol. Fertil. Soils*, 33(1), 17-24. <https://doi.org/10.1007/s003740000281>
- Qu, Q., Zhang, J., Hai, X., Wu, J., Fan, J., Wang, D., Li, J., Shanguan, Z. and Deng, L. (2022). Long-term fencing alters the vertical distribution of soil $\delta^{13}C$ and SOC turnover rate: Revealed by MBC- $\delta^{13}C$. *Agric. Ecosyst. Environ.*, 339, 108119. <https://doi.org/10.1016/j.agee.2022.108119>
- Rao, Z., Chen, F., Zhang, X., Xu, Y., Xue, Q. and Zhang, P. (2012). Spatial and temporal variations of C₃/C₄ relative abundance in global terrestrial ecosystem since the Last Glacial and its possible driving mechanisms. *Chin. Sci. Bull.*, 57(31), 4024-4035. <https://doi.org/10.1007/s11434-012-5233-9>
- Rao, Z., Guo, W., Cao, J., Shi, F., Jiang, H. and Li, C. (2017). Relationship between the stable carbon isotopic composition of modern plants and surface soils and climate: A global review. *Earth Sci. Rev.*, 165, 110-119. <https://doi.org/10.1016/j.earscirev.2016.12.007>
- Scharlemann J.P.W., Tanner, E.V.J., Hiederer, R. and Kapos, V. (2014). Global soil carbon: understanding and managing the largest terrestrial carbon pool. *Carbon Manage.*, 5(1), 81-91. <https://doi.org/10.4155/cmt.13.77>
- Shi, Z., Crowell, S., Luo, Y. and Moore III, B. (2018). Model structures amplify uncertainty in predicted soil carbon responses to climate change. *Nat. Commun.*, 9(1), 2171. <https://doi.org/10.1038/s41467-018-04526-9>
- Singh, G., and Panda, R.K. (2011). Daily sediment yield modeling with artificial neural network using 10-fold cross validation method: a small agricultural watershed, Kappari, India. *Int. J. Earth Sci. Eng.*, 4(06), 443-450.
- Singhal, M., Gairola, A.C. and Singh, N. (2021). Artificial neural network-assisted glacier forefield soil temperature retrieval from temperature measurements. *Theor. Appl. Climatol.*, 143(3-4), 1157-1166. <https://doi.org/10.1007/s00704-020-03498-5>
- Sollins, P., Kramer, M.G., Swanston, C., Lajtha, K., Filley, T., Auf-

- denkampe, A.K., Wagai, R. and Bowden, R.D. (2009). Sequential density fractionation across soils of contrasting mineralogy: evidence for both microbial- and mineral-controlled soil organic matter stabilization. *Biogeochemistry*, 96(1-3), 209-231. <https://doi.org/10.1007/s10533-009-9359-z>
- Song, W. and Zhou, Y. (2021). Linking leaf $\delta^{15}\text{N}$ and $\delta^{13}\text{C}$ with soil fungal biodiversity, ectomycorrhizal and plant pathogenic abundance in forest ecosystems of China. *CATENA*, 200, 105176. <https://doi.org/10.1016/j.catena.2021.105176>
- Sun, Y., Feng, Y., Wang, Y., Zhao, X., Yang, Y., Tang, Z., Wang, S., Su, H., Zhu, J., Chang, J. and Fang, J. (2021). Field-Based Estimation of Net Primary Productivity and Its Above- and Belowground Partitioning in Global Grasslands. *J. Geophys. Res. Biogeosci.*, 126(11). <https://doi.org/10.1029/2021jg006472>
- Tang, X., Fan, S., Du, M., Zhang, W., Gao, S., Liu, S., Chen, G., Yu, Z. and Yang, W. (2020). Spatial and temporal patterns of global soil heterotrophic respiration in terrestrial ecosystems. *Earth Syst. Sci. Data*, 12(2), 1037-1051. <https://doi.org/10.5194/essd-12-1037-2020>
- Tang, X., Fan, S., Zhang, W., Gao, S., Chen, G. and Shi, L. (2019). Global variability in belowground autotrophic respiration in terrestrial ecosystems. *Earth Syst. Sci. Data*, 11(4), 1839-1852. <https://doi.org/10.5194/essd-11-1839-2019>
- R Core Team (2022). R: A language and environment for statistical computing. R Foundation for Statistical Computing, Vienna, Austria. More information is available at <https://cran.r-project.org/bin/windows/base/old/4.2.1/README.R-4.2.1>
- Tieszen, L.L., Reed, B.C., Bliss, N.B., Wylie, B.K. and DeJong, D.D. (1997). N₂O, C₃ and C₄ productivity, and distributions in great plains grassland land cover classes. *Ecol. Appl.*, 7(1), 59-78. [https://doi.org/10.1890/1051-0761\(1997\)007\[0059:NCACPA\]2.0.CO;2](https://doi.org/10.1890/1051-0761(1997)007[0059:NCACPA]2.0.CO;2)
- Van Groenigen, K.J., Qi, X., Osenberg, C.W., Luo, Y.Q. and Hungate, B.A. (2014). Faster Decomposition Under Increased Atmospheric CO₂ Limits Soil Carbon Storage. *Science*, 344(6183), 508-509. <https://doi.org/10.1126/science.1249534>
- Volk, M., Bassin, S., Lehmann, M.F., Johnson, M.G. and Andersen, C.P. (2018). ^{13}C isotopic signature and C concentration of soil density fractions illustrate reduced C allocation to subalpine grassland soil under high atmospheric N deposition. *Soil Biol. Biochem.*, 125, 178-184. <https://doi.org/10.1016/j.soilbio.2018.07.014>
- Wan, Z., Hook, S., and Hulley, G. (2021). MODIS/Terra Land Surface Temperature/Emissivity 8-Day L3 Global 1km SIN Grid V061 [Dataset]. NASA EOSDIS Land Processes DAAC. <https://doi.org/10.5067/MODIS/MOD11A2.061>
- Wang, Luo, Lu, Houyuan, Wu, Naiqin, Chu, Duo, Han, and Bulletin, J.J.C.S. (2004). Discovery of C₄ species at high altitude in Qinghai-Tibetan Plateau. *Chin. Sci. Bull.*, 49(13), 1392-1396. <https://doi.org/10.1007/BF03036887>
- Wang, C., Houlton, B.Z., Liu, D., Hou, J., Cheng, W. and Bai, E. (2018). Stable isotopic constraints on global soil organic carbon turnover. *Biogeosciences*, 15(4), 987-995. <https://doi.org/10.5194/bg-15-987-2018>
- Wang, C., Wei, H., Liu, D., Luo, W., Hou, J., Cheng, W., Han, X. and Bai, E. (2017). Depth profiles of soil carbon isotopes along a semi-arid grassland transect in northern China. *Plant Soil*, 417(1-2), 43-52. <https://doi.org/10.1007/s11104-017-3233-x>
- Wang, G.A., Li, J.Z., Liu, X.Z. and Li, X.Y. (2013). Variations in carbon isotope ratios of plants across a temperature gradient along the 400 mm isohet of mean annual precipitation in north China and their relevance to paleovegetation reconstruction. *Quat. Sci. Rev.*, 63, 83-90. <https://doi.org/10.1016/j.quascirev.2012.12.004>
- Wang, S., Fan, J., Song, M., Yu, G., Zhou, L., Liu, J., Zhong, H., Gao, L., Hu, Z., Wu, W. and Song, T. (2012). Patterns of SOC and soil ^{13}C and their relations to climatic factors and soil characteristics on the Qinghai-Tibetan Plateau. *Plant Soil*, 363(1-2), 243-255. <https://doi.org/10.1007/s11104-012-1304-6>
- Wu, G., Liu, H., Hua, L., Luo, Q., Lin, Y., He, P., Feng, S., Liu, J. and Ye, Q. (2018). Differential Responses of Stomata and Photosynthesis to Elevated Temperature in Two Co-occurring Subtropical Forest Tree Species. *Front. Plant Sci.*, 9. <https://doi.org/10.3389/fpls.2018.00467>
- Wynn, J.G., Bird, M.I., Vellen, L., Grand-Clement, E., Carter, J. and Berry, S.L. (2006). Continental-scale measurement of the soil organic carbon pool with climatic, edaphic, and biotic controls. *Global Biogeochem. Cy.*, 20(1). <https://doi.org/10.1029/2005gb002576>
- Wynn, J.G., Harden, J.W. and Fries, T.L. (2006). Stable carbon isotope depth profiles and soil organic carbon dynamics in the lower Mississippi Basin. *Geoderma*, 131(1-2), 89-109. <https://doi.org/10.1016/j.geoderma.2005.03.005>
- Xu, M. and Shang, H. (2016). Contribution of soil respiration to the global carbon equation. *J. Plant Physiol.*, 203, 16-28. <https://doi.org/10.1016/j.jplph.2016.08.007>
- Xu, X., Shi, Z., Li, D., Rey, A., Ruan, H., Craine, J.M., Liang, J., Zhou, J. and Luo, Y. (2016). Soil properties control decomposition of soil organic carbon: Results from data-assimilation analysis. *Geoderma*, 262, 235-242. <https://doi.org/10.1016/j.geoderma.2015.08.038>
- Yamazaki, D., Ikeshima, D., Tawatari, R., Yamaguchi, T., O'Loughlin, F., Neal, J.C., Sampson, C.C., Kanae, S. and Bates, P.D. (2017). A high-accuracy map of global terrain elevations. *Geophys. Res. Lett.*, 44(11), 5844-5853. <https://doi.org/10.1002/2017gl072874>
- Yang, X., Lin, L., Li, Y. and He, J. (2017). Effects of Warming and Altered Precipitation on Soil Physical Properties and Carbon Pools in a Tibetan Alpine Grassland. *Beijing Da Xue Xue Bao*, 53(4), 765-774. <https://link.cnki.net/doi/10.13209/j.0479-8023.2017.086>
- Yang, Y., Ji, C., Chen, L., Ding, J., Cheng, X., Robinson, D. and Whitehead, D. (2015). Edaphic rather than climatic controls over ^{13}C enrichment between soil and vegetation in alpine grasslands on the Tibetan Plateau. *Funct. Ecol.*, 29(6), 839-848. <https://doi.org/10.1111/1365-2435.12393>
- Yang, Y.H., Fang, J.Y., Smith, P., Tang, Y.H., Chen, A.P., Ji, C.J., Hu, H.F., Rao, S., Tan, K. and He, J.S. (2009). Changes in topsoil carbon stock in the Tibetan grasslands between the 1980s and 2004. *Glob. Change Biol.*, 15(11), 2723-2729. <https://doi.org/10.1111/j.1365-2486.2009.01924.x>
- Yang, Z., Luo, X., Shi, Y., Zhou, T., Luo, K., Lai, Y., Yu, P., Liu, L., Olchev, A., Bond-Lamberty, B., Hao, D., Jian, J., Fan, S., Cai, C. and Tang, X. (2023). Controls and variability of soil respiration temperature sensitivity across China. *Sci. Total Environ.*, 871, 161974. <https://doi.org/10.1016/j.scitotenv.2023.161974>
- Yao, Y., Wang, X., Li, Y., Wang, T., Shen, M., Du, M., He, H., Li, Y., Luo, W., Ma, M., Ma, Y., Tang, Y., Wang, H., Zhang, X., Zhang, Y., Zhao, L., Zhou, G. and Piao, S. (2018). Spatiotemporal pattern of gross primary productivity and its covariation with climate in China over the last thirty years. *Glob. Change Biol.*, 24(1), 184-196. <https://doi.org/10.1111/gcb.13830>
- Zhang, D., Yang, Y. and Ran, M. (2020). Variations of surface soil $\delta^{13}\text{C}_{\text{org}}$ in the different climatic regions of China and paleoclimatic implication. *Quatern. Int.*, 536, 92-102. <https://doi.org/10.1016/j.quaint.2019.12.015>
- Zhang, Y., Kong, D., Gan, R., Chiew, F.H.S., McVicar, T.R., Zhang, Q. and Yang, Y. (2019). Coupled estimation of 500 m and 8-day resolution global evapotranspiration and gross primary production in 2002-2017. *Remote Sens. Environ.*, 222, 165-182. <https://doi.org/10.1016/j.rse.2018.12.031>
- Zhang, Z.H., Zhao, M.X., Lu, H.Y. and Faiia, A.M. (2003). Lower temperature as the main cause of C-4 plant declines during the glacial periods on the Chinese Loess Plateau. *Earth Planet. Sci. Lett.*, 214(3-4), 467-481. [https://doi.org/10.1016/S0012-821x\(03\)00387-X](https://doi.org/10.1016/S0012-821x(03)00387-X)
- Zhao, Y., Wang, X., Ou, Y., Jia, H., Li, J., Shi, C. and Liu, Y. (2019). Variations in soil $\delta^{13}\text{C}$ with alpine meadow degradation on the eastern Qinghai-Tibet Plateau. *Geoderma*, 338, 178-186. <https://doi.org/10.1016/j.geoderma.2018.12.005>
- Zhao, Y., Wu, F., Fang, X. and Yang, Y. (2017). Altitudinal variations

- in the bulk organic carbon isotopic composition of topsoil in the Qilian Mountains area, NE Tibetan Plateau, and its environmental significance. *Quatern. Int.*, 454, 45-55. <https://doi.org/10.1016/j.quaint.2017.08.045>
- Zheng, L. and Song, W. (2022). Phosphorus Limitation of Trees Influences Forest Soil Fungal Diversity in China. *Forests*, 13(2), 223. <https://doi.org/10.3390/f13020223>
- Zhou, T., Hou, Y., Yang, Z., Laffitte, B., Luo, K., Luo, X., Liao, D. and Tang, X. (2023). Reducing spatial resolution increased net primary productivity prediction of terrestrial ecosystems: A Random Forest approach. *Sci. Total Environ.*, 165134. <https://doi.org/10.1016/j.scitotenv.2023.165134>
- Zhou, X., Xin, J., Huang, X., Li, H., Li, F. and Song, W. (2022). Linking Leaf Functional Traits with Soil and Climate Factors in Forest Ecosystems in China. *Plants*, 11(24), 3545. <https://doi.org/10.3390/plants11243545>
- Zhou, Y., Zhang, W., Cheng, X., Harris, W., Schaeffer, S.M., Xu, X. and Zhao, B. (2019). Factors affecting ^{13}C enrichment of vegetation and soil in temperate grasslands in Inner Mongolia, China. *J. Soils Sediments*, 19(5), 2190-2199. <https://doi.org/10.1007/s11368-019-02248-z>
- Zhou, Z., Liu, L. and Hou, L. (2022). Soil organic carbon stabilization and formation: mechanism and model. *J. Beijing For. Univ.*, 44(10), 11. <https://doi.org/10.12171/j.1000-1522.20220183>